Surface-Enhanced Resonance Raman Scattering and Density Functional Calculations of Hemicyanine Adsorbed on Colloidal Silver Surface

N. Biswas,*,† S. Thomas,‡ S. Kapoor,*,† A. Mishra,§ S. Wategaonkar,§ S. Venkateswaran,‡ and T. Mukherjee†

Radiation & Photochemistry Division, Bhabha Atomic Research Centre, Mumbai 400085, India, Synchrotron Radiation Section, Bhabha Atomic Research Centre, Mumbai 400085, India, and Department of Chemical Sciences, Tata Institute of Fundamental Research, Mumbai 400005, India

Received: September 20, 2005; In Final Form: December 13, 2005

Resonance Raman (RR) and surface-enhanced resonance Raman scattering (SERRS) of 4′-(*N*,*N*′-dimethylaminostyryl)-4-propylpyridinium bromide (hemicyanine, HC dye) in acetonitrile solution and on a colloidal silver surface have been investigated. The structure of the dye in the ground (S_0) and excited (S_1) electronic states was optimized using density functional calculations along with the B3LYP and the configuration interaction with the singlet excitation (CIS) methods, respectively, using the 6-31G* basis set. The vibrational frequencies of the molecule were computed at the optimized geometry and compared with the observed Raman bands. A complete normal-mode analysis has been carried out because it is essential for the accurate assignment of the vibrational spectra. From the observed enhancement along various in-plane and out-of-plane vibrations in the SERRS spectrum and from theoretical calculations, it has been inferred that the interaction with the silver surface occurs via the nitrogen lone pair of the pyridyl or the dimethylamino group of the molecule with a tilted orientation. The observed red-shifts in the SERRS spectrum along various vibrations indicate strong interaction (chemisorption) of the HC dye with the silver surface. This is also supported by the presence of a Ag−N stretching vibration at 241 cm^{-1}. The effect of the dye concentration on the orientation of the molecule is also discussed.

1. Introduction

Resonance Raman (RR) spectroscopy is a powerful technique for extracting valuable information regarding the changes associated with the nuclear motion of a molecule following electronic excitation.[1−6] The RR frequencies reflect the geometry of the molecule in the ground electronic state. Under preresonance or resonance conditions, the Raman bands gain intensity and, thus, reflect the excited-state geometry change upon electronic excitation. Often during the study of RR in solution, due to the high fluorescence quantum yield of the system under investigation, the weak Raman signals are completely masked by the fluorescence background and, hence, do not give meaningful information. Under these conditions, the technique of choice is surface-enhanced Raman scattering[7−9] (SERS), where due to adsorption of the molecule onto the metal surface, the fluorescence background is reduced followed by the enhancement of Raman intensities. SERS has become an increasingly popular technique not only for studying the molecules or ions at trace concentrations but also in estimating their possible orientations on the metal surfaces.[10−15] An important aspect of SERS is its potential for probing the interaction between various adsorbates and metallic surfaces. The application of "surface selection rules"[16] helps in providing information on the sites of binding and the molecular orientation on the metal surface.

Surface-enhanced resonance Raman spectroscopy[17] (SERRS), which is a combination of SERS and RRS, has major advantages over the latter techniques; namely, it can be used to study wide concentration ranges, and the detection limit is orders of magnitude below monolayer coverage; i.e., its sensitivity is comparable to or better than that of fluorescence. The SERRS technique also has the advantage of overcoming the problem of fluorescence in solution, in addition to providing vibrational information on the adsorbate. It is also possible to obtain electronic information through the excitation profiles obtained from SERRS.

Hemicyanine (HC) dyes are characterized by the presence of two nitrogen atoms, one of which is positively charged and acts as an electron acceptor and the other with a lone pair of electrons that acts as a donor. HC dyes thus exhibit solvent-dependent emission properties and have been widely used as fluorescent probes in biochemistry and biophysics.[18−21] These dyes also undergo intramolecular charge transfer, have large first-order hyperpolarizability (β),[22−24] and are useful in the study of nonlinear optical devices[25] and molecular electronics.[26] These dyes have also been widely used in industries as spectral sensitizers for silver-halide photography in optical disks as recording media, as photorefractive materials, in laser devices, as antitumor reagents, and as molecular aggregates.[27] Absorption, RR[1] spectra, and fluorescence lifetimes of 4′-(*N*,*N*′-dimethylaminostyryl)-4-alkylpyridinium) salts of varying alkyl chain lengths[28] and their aggregates[29] have been measured in different organic solvents. A detailed vibrational assignment of the 4′-(*N*,*N*′-dimethylaminostyryl)-4-propylpyridinium bromide and its structural characterization is not available in the literature. Moreover, in the reports on SERS of methyl pyridinium salt[30]

* To whom correspondence should be addressed. Dr. Nandita Biswas (E-mail: nanbis@yahoo.com; nanditab@apsara.barc.ernet.in). Dr. Sudhir Kapoor (E-mail: sudhirk@apsara.barc.ernet.in). Fax: (+) 91-22-25505151. Phone: (+) 91-22-25590298.

† Radiation & Photochemistry Division.

‡ Synchrotron Radiation Section.

§ Tata Institute of Fundamental Research.

10.1021/jp055330q CCC: $33.50
Published on Web 01/07/2006

SCHEME 1

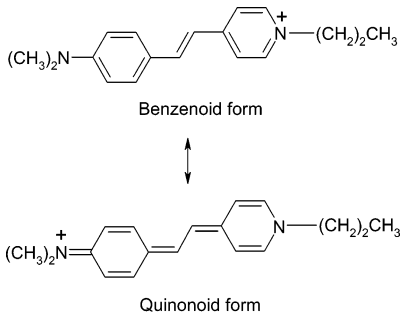

and the *n*-docosyl homologue of HC[31] as well as Langmuir−Blodgett films deposited on a copper surface, the assignments of various normal modes are found to be in disagreement with the present investigation.

In this article, we report the RR and SERRS spectra of HC {4′-(*N*,*N*′-dimethylaminostyryl)-4-propylpyridinium bromide} in acetonitrile solution and on a colloidal silver surface. HC represents a donor−acceptor system that can exist in a resonance balance between benzenoid and quinonoid forms, as shown in Scheme 1. The aim of the present study is as follows: (1) to elucidate the detailed structural and vibrational characteristics of HC using electronic absorption, RRS, and SERRS techniques; (2) to assign the observed Raman vibrations using the calculated vibrational frequencies; (3) to probe the interaction/orientation of HC on the silver surface as seen from the enhancement and shifts in the SERRS spectra and from theoretical calculations; and (4) to study the effect of HC concentration on the SERRS spectra.

2. Experimental Section

4′-(*N*,*N*′-dimethylaminostyryl)-4-propylpyridinium bromide (HC) was prepared by the reaction of *n*-propylbromide with γ-picoline followed by Knoevenagel condensation with dimethylaminobenzaldehyde following a method reported in the literature.[32,33] Acetonitrile, used for the Raman measurements, was bought from SISCO Research Laboratories, India, and was used without further purification. The UV−visible absorption spectra were recorded using a Chemito UV2600 spectrophotometer. For the RR measurements, the samples of HC in acetonitrile were taken in a capillary tube and were excited using 457.9, 476.5, 488, and 514.5 nm lines of a Coherent Ar^+ laser, and the laser powers used were 50, 60, 100, and 90 mW, respectively. The Raman scattered light was collected at 90° using a SPEX Ramalog double monochromator (model 1401). The spectrometer was operated in the photon-counting mode, and a PC-based system was used for data acquisition and monochromator control. For SERRS, colloidal silver sol was prepared by the reduction of silver nitrate with sodium borohydride using the method of Creighton et al.[34] The size of the silver particles in the colloid was determined to be 15−20 nm using TEM studies.[35] Water purified by a Millipore system was used for the preparation of silver sol. The SERRS measurements were carried out at pH $\approx$ 9 using the 514.5 nm line of a Coherent Ar^+ laser. The laser power at the sample was 90 mW at 514.5 nm. The Raman scattered light was collected similar to that mentioned above for the RR measurements. For the RR and SERRS measurements, a defocused beam was used to impair thermal effects. The RR and SERRS signals were found to be linear with an incident laser power of 30−90 mW. Each measurement was repeated several times to ensure reproducibility. Moreover, the absorption spectra of the irradiated sample were also checked to ensure that no photodegradation or photoproducts were formed during irradiation with the laser beam.

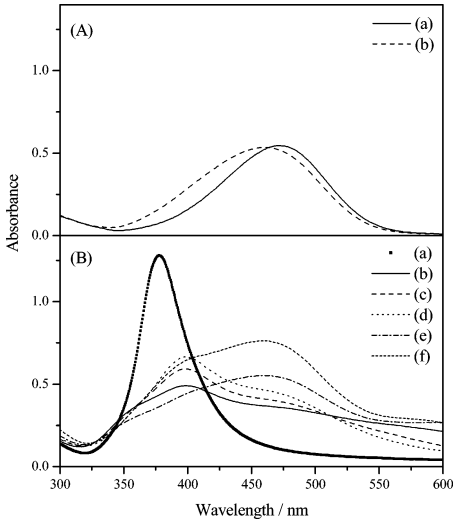

Figure 1. (A) UV−vis absorption spectra of (a) HC in acetonitrile and (b) HC in 10% acetonitrile in water. (B) UV−vis absorption spectrum of (a) pure silver hydrosol, and with added HC at (b) 8×10^{-6}, (c) 1.0×10^{-5}, (d) 1.3×10^{-5}, (e) 1.6×10^{-5}, and (f) 2.4×10^{-5} M.

3. Computational Details

To get an insight into the experimental results, the structure of HC in its ground (S_0) and excited (S_1) electronic states was computed using the density functional theoretical (DFT) and the configuration interaction with singlet excitation (CIS) methods with Gaussian 98 program package.[36] The DFT calculations were carried out with Becke's three-parameter hybrid method using the Lee−Yang−Parr correlation functional (abbreviated as B3LYP[37]). The 6-31G* Pople split-valence polarization basis set was used for the geometry optimization. This basis set is sufficiently complete to permit a good description of the wave function and has been known to work reasonably well for large polyatomic systems.[38,39] For the HC−Ag complex, the LANL2DZ basis set was used. No symmetry restriction was applied during geometry optimization. The vibrational frequencies were computed at the optimized geometry to ensure that no imaginary frequencies were obtained confirming that it corresponds to a local minimum on the potential-energy surface and not to a saddle point.

4. Results and Discussion

4.1. UV−Vis Absorption Spectra. The UV−vis absorption spectra of HC in acetonitrile and in 10% acetonitrile in water are shown in Figure 1A (a and b, respectively). The absorption band of HC, which is attributed to the charge-transfer transition, shows a maxima at 471 and 461 nm in acetonitrile and 10% acetonitrile in water, respectively. HC, in its ground electronic state, is known to exist in a trans configuration around the central C═C bond. In the ground (S_0) state, it has a positive charge centered on the pyridyl ring, whereas in the excited (S_1) state, the charges are more evenly distributed.[40] With the excited state of HC being less polar in nature as compared to the ground state, the absorption maxima shifts to the blue with an increase in solvent polarity. HC thus exists in a resonance balance between the benzenoid and quinonoid forms, as shown in Scheme 1. In the ground state, the benzenoid form dominates,

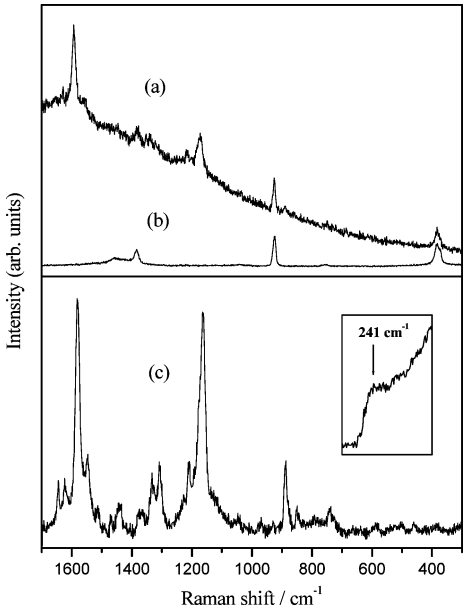

Figure 2. (a) RR spectrum of HC in acetonitrile at excitation wavelength 457.9 nm; (b) normal Raman spectrum of acetonitrile at 457.9 nm; (c) SERR spectrum of HC adsorbed on silver hydrosol at 514.5 nm. (Inset) Ag−N stretching vibration at 241 cm^{-1}.

whereas the quinonoid form dominates in the excited state. The electronic excitation from the ground to the excited state, which involves a change from the benzenoid to the quinonoid form, is thus expected to be accompanied by significant changes in the central C═C bond and the pyridyl and aniline rings connected to the central C═C bond.

4.2. Resonance Raman (RR) Spectra. The Raman spectrum of the HC dye in acetonitrile (2×10^{-4} M) in resonance with the lowest energy-absorption spectrum recorded at 457.9-nm excitation is shown in Figure 2a. In Figure 2b is shown the Raman spectrum of the solvent acetonitrile. A comparison of the two spectra shows that apart from the acetonitrile peaks appearing at 381, 922, 1374, and 1452 cm^{-1}, two strong peaks were observed for HC at 1167 and 1586 cm^{-1}. Weak peaks of HC were also observed at 887, 1212, 1331, 1375, 1441, 1548, 1622, and 1648 cm^{-1}. The experimentally observed vibrations are tabulated in Table 1. The observed frequencies are assigned on the basis of the normal modes obtained from DFT calculations.

In Figure 3a−c, the RR spectra of HC are shown as a function of the excitation wavelength, viz. 457.9, 476.5, and 488 nm. All of the Raman spectra were normalized with respect to the solvent band observed at 922 cm^{-1}. From the figure, it is observed that at the excitation wavelengths, 457.9, 476.5, and 488 nm (these wavelengths are in resonance with the absorption band corresponding to the charge-transfer transition) along with an increase in the fluorescence background, the vibrations corresponding to 1167 and 1586 cm^{-1} show maximum intensity and, hence, must be coupled to the charge-transfer transition. The RR spectrum recorded using 514.5-nm excitation is not shown due to the huge fluorescence background. Due to the interference from the fluorescence background, absolute RR intensity analysis could not be carried out. The experimentally observed frequencies are assigned on the basis of the computed vibrations, as shown below.

4.3. Computational Results. The trans conformer of HC in the ground (S_0) and excited (S_1) electronic states were optimized using DFT (B3LYP/6-31G*) and CIS/6-31G* methods. The ground-state geometry of *trans*-HC, optimized at the B3LYP/6-31G* level, is shown in Figure 4 along with the atom numbering. To have a better understanding of the structure of the molecule, the bond lengths of the S_0 and S_1 electronic states are included in Table 2. It is seen from the table that C_2C_1 has a bond length of 1.375 (1.393) Å whereas C_3C_1 and C_4C_2 have bond lengths of 1.428 (1.412) and 1.426 (1.411) Å in the S_0 and (S_1) electronic states, respectively. The pyridyl and aniline rings also have varying bond lengths. Thus, HC exists in the benzenoid form in its ground electronic state and shifts toward the quinonoid form in its excited electronic state.

The B3LYP vibrational frequencies with the 6-31G* basis set for HC in vacuum were slightly overestimated and were scaled by a factor of 0.97 to get a better agreement with the experimental frequencies. For a one-to-one correspondence of the calculated vibrations with the observed RR frequencies, the calculated Raman intensities were also taken into account. For the sake of comparison, we have also included the IR and Raman data obtained from the literature for the hemicyanine dye (methyl pyridinium iodide[1]) in solid KBr. The most intense Raman bands observed in the RR spectra at 1586 and 1167 cm^{-1} have been assigned to ethylene C_2C_1 and $C_{34}N_{33}$ stretching vibrations, respectively. The former Raman band has contributions from the aniline ring CC stretch, C_3C_1 stretch, and ethylene HCC in-plane (ip) bend, and the latter band is in combination with the pyridyl ring CC stretch and the pyridyl HCC ip bend. Thus, on resonance excitation to the lowest energy state, the HC molecule undergoes maximum displacement along the C_2C_1, $C_{34}N_{33}$, C_3C_1, aniline, and pyridyl ring coordinates. The weak band observed in the RR spectra at 887 cm^{-1} is assigned to the pyridyl ring-breathing mode in combination with the ethylene CCC ip bend and aniline ring deformation. This assignment is in disagreement with that reported previously in the literature (methyl pyridinium iodide[1,30] and *n*-docosyl homologue of hemicyanine[31]). The previous reports have assigned this mode to the ethylene H out-of-plane (oop) bend. In Figure 5a we have shown the normal-mode displacement picture for the 887 cm^{-1} vibration, which clearly is in agreement with our assignment. The other weak modes are observed at 1212, 1331, 1375, 1441, 1548, 1622, and 1648 cm^{-1}. Of these vibrations, the 1212 and 1331 cm^{-1} modes are assigned to pyridyl ring HCC ip bends. The 1375, 1441, 1548, 1622, and 1648 cm^{-1} modes are assigned to a $HC_{34}N_{33}$ ip bend, HCN_{14} methyl bend, $C_{13}N_{14}$ stretch, aniline ring (CC) stretch, and pyridyl ring (CC) stretch, respectively. The normal-mode displacements of 1167, 1586, and 1648 cm^{-1} vibrations are also included in Figure 5b−d.

The silver complex of the *trans*-HC conformer was optimized using B3LYP with the LANL2DZ basis set. Two possible conformers were obtained. In conformer I, Ag is in proximity to the pyridinium moiety, whereas in conformer II, it is close to the dimethylamino group, as shown in Figure 6a,b. Conformer I is found to be slightly more stable (∼138 cm^{-1}) with respect to conformer II. The schematic model for the adsorption of *trans*-HC on the silver surface (Figure 6) will be discussed later in the section of SERRS. For both conformers of the HC−Ag complex, the vibrational frequencies were computed at the optimized geometry to ensure that no imaginary frequencies were obtained. The calculated frequencies for both of the conformers were within a few wavenumbers and were scaled by a factor of 0.97 to have a good agreement with the observed SERRS vibrations. The calculated frequencies for conformer I of the HC−Ag complex are included in Table 1.

4.4. UV−Vis Absorption Spectra in Colloidal Silver. The UV−visible absorption spectrum of colloidal silver sol (solid squares) is shown in Figure 1B (a). The silver sol shows a single

TABLE 1: Assignment of IR, Normal Raman, RR, SERRS, and Calculated Vibrations of HC and HC−Ag Complex (Conformer I) in cm^{-1} [a]

IR[b]	Raman[b]	RR[c]	SERRS[c]	calcd[d]	calcd[e]	approximate assignments
1643 m	1641 m	1648 w	1640 s	1656	1642	$\upsilon(CC)_{py} + \delta(HCC)_{py}$
	1613 m	1622 w	1617 s	1633	1627	$\upsilon(CC)_{ani} + \delta(HCC)_{ani} + \upsilon(C_2C_1)$
1580 s	1575 s	1586 s	1578 s	1574	1569	$\upsilon(C_2C_1) + \upsilon(CC)_{ani} + \delta(HCC)_{eth} + \upsilon(C_3C_1)$
1544 w	1541 w	1548 w	1543 m	1540	1534	$\upsilon(C_{13}N_{14}) + \upsilon(CC)_{ani} + \delta(HCC)_{ani}$
1508 m	1510 w		1507 w	1513	1506	$\delta(HCC)_{py} + \upsilon(CC)_{py}$
1466 m	1467 w		1466 m	1461	1471	$\upsilon(CC)_{ani} + \delta(HCC)_{ani}$
1447 w		1441 w	1434 w	1428	1454	$\delta(HCN_{14})_{me}$
1372 m	1363 m	1375 m	1370 m	1358	1384	$\delta(HC_{34}N_{33}) + \delta(HCC)_{pr}$
1331 w	1328 w	1331 m	1327 m	1317	1323	$\delta(HCC)_{py} + \upsilon(C_{eth}C_{Ph}) + \upsilon(CC)py$
1304 m	1303 m		1303 m	1298	1296	$\delta(HCC)_{eth} + \upsilon(C_2C_1)$
1225 m	1219 m	1212 m	1206 m	1208	1218	$\delta(HCC)_{py} + \upsilon(CC)_{py} + \delta(HCC)_{eth}$
1177 s	1176 s	1167 s	1161 s	1160	1156	$\upsilon(C_{34}N_{33}) + \upsilon(py) + \delta(HCC)_{py}$
1040 m	1039 w		1049 w	1027	1022	$\upsilon(CC)_{me} + \delta(HCC)_{py}$
975 m	976 w		970 w	933	924	$\upsilon(C_{me}N_{14}) + \upsilon(CC)_{ani}$
871 m	880 s	887 w	883 m	869	865	$\upsilon(CC)_{py} + \delta(CC_{eth}C_{eth}) + \upsilon(CC)_{ani}$
851 w	846 w		848 m	819	836	$\gamma(CH)_{ani} + \gamma(CH)_{py} + \gamma(CH)_{eth}$
728 w			738 m	728	723	$\upsilon(C_{me}N_{14}) + \tau(C_{35}C_{34}) + \upsilon(CC)_{ani} + \upsilon(C_{34}N_{33})$
572 w	570 m		585 w	574	574	$\delta(CC_{eth}C_{eth}) + \delta(C_{35}C_{34}N_{33}) + \tau(C_{34}C_{35})$
536 m			545 w	532	540	$\gamma(C-H)_{me} + \tau(C_{34}N_{33}) + \tau(C_4C_2)$
500 w	500 m		501 w	497	500	$\delta(CN_{14}C_{13}) + \delta(C_{ani}C_{ani}C_{eth}) + \delta(C_{py}C_{py}C_{eth}) + \delta(CC_{eth}C_{eth})$
	458 m		459 w	453	453	$\delta(C_{py}C_{py}C_{eth}) + \delta(C_{me}N_{14}C_{13}) + \tau(C_{me}N_{14}) + \tau(C_{34}N_{33})$
			241 sh		260	$\upsilon(Ag-N)$

[a] Abbreviations used: eth: ethylene; py: pyridyl ring; ani: aniline ring; pr: propyl group, me: methyl group. s: strong, m: medium, w: weak; sh: shoulder. [b] Methyl pyridinium iodide in solid KBr.[1] [c] Present work. [d] B3LYP/6-31G* calculated frequencies for HC in vacuum scaled by a factor of 0.97. [e] B3LYP/LANL2DZ calculated frequencies for HC−Ag complex scaled by a factor of 0.97.

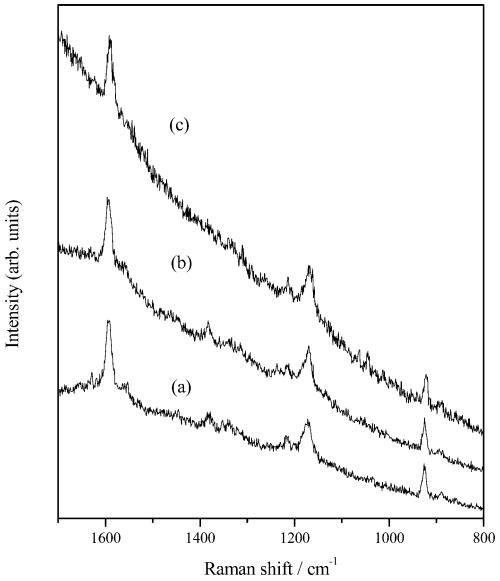

Figure 3. RR spectrum of HC in acetonitrile at excitation wavelengths (a) 457.9, (b) 476.5, and (c) 488 nm.

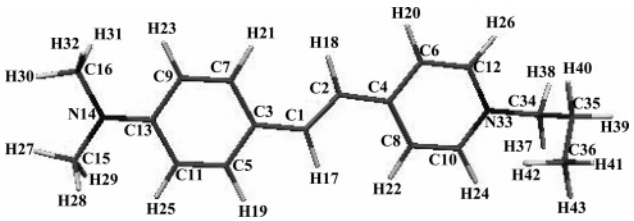

Figure 4. Trans-conformer of 4′-(*N*,*N*′-dimethylaminostyryl)-4-propylpyridinium bromide (HC) optimized at the B3LYP/6-31G* level along with the atom numbering.

sharp peak with maximum at 377 nm, which is due to the surface plasmon absorption band. The absorption spectra of the hemicyanine dye at various concentrations in the sol (8×10^{-6}, 1.0×10^{-5}, 1.3×10^{-5}, 1.6×10^{-5}, and 2.4×10^{-5} M) are also shown in Figure 1B (b−f). It is observed that with the addition of the HC dye to the silver sol, the absorption spectrum becomes very broad with a decrease in the absorbance of the surface plasmon band, which is also shifted toward 398 nm (attributed to aggregated silver nanoparticles) and the appearance of a new band around 480−500 nm that is ascribed to the metal−molecule charge-transfer interaction At higher concentrations of the HC dye [Figure 1B (e,f)], the absorption spectrum shows some amount of free HC molecules remaining in solution, which is evident from the increase in its corresponding peak intensity (around 460 nm).

TABLE 2: Optimized Bond Lengths (Å) of HC in the Ground (S_0) and Excited (S_1) Electronic States

bond lengths	B3LYP 6-31G*	CIS 6-31G*	bond lengths	B3LYP 6-31G*	CIS 6-31G*
C_2C_1	1.375	1.393	$C_{13}C_9$	1.428	1.427
C_3C_1	1.428	1.412	$C_{13}C_{11}$	1.425	1.430
C_4C_2	1.426	1.411	$C_{10}N_{33}$	1.364	1.354
C_5C_3	1.418	1.428	$C_{12}N_{33}$	1.364	1.362
C_6C_4	1.426	1.427	$C_{13}N_{14}$	1.361	1.342
C_7C_3	1.420	1.429	$C_{15}N_{14}$	1.462	1.457
C_8C_4	1.426	1.431	$C_{16}N_{14}$	1.462	1.457
C_9C_7	1.375	1.359	$C_{34}N_{33}$	1.484	1.471
$C_{10}C_8$	1.370	1.354	$C_{35}C_{34}$	1.534	1.530
$C_{11}C_5$	1.377	1.357	$C_{36}C_{35}$	1.531	1.528
$C_{12}C_6$	1.370	1.352			

4.5. Surface-Enhanced Resonance Raman Scattering (SERRS). The SERRS spectrum of HC (1.6×10^{-5} M) in silver hydrosol, measured using 514.5 nm excitation in the region of 200−1700 cm^{-1}, is shown in Figure 2c. A comparison of the SERRS spectrum with the RR spectrum shows a relative enhancement of various ip bending and stretching vibrations and a few oop bending vibrations in the region of 400−1700 cm^{-1}. The vibrations observed in the SERRS spectrum are included in Table 1. Similar to the RRS, the most intense bands in the SERRS appear at 1161 and 1578 cm^{-1}, but these are red-shifted by 6−8 cm^{-1}. Other Raman bands, which were observed to be of weak intensity in the RRS, gain moderate intensity in the SERRS spectrum viz. 883, 1206, 1327, 1370, 1434, 1543, 1617, and 1640 cm^{-1} modes. In addition to these

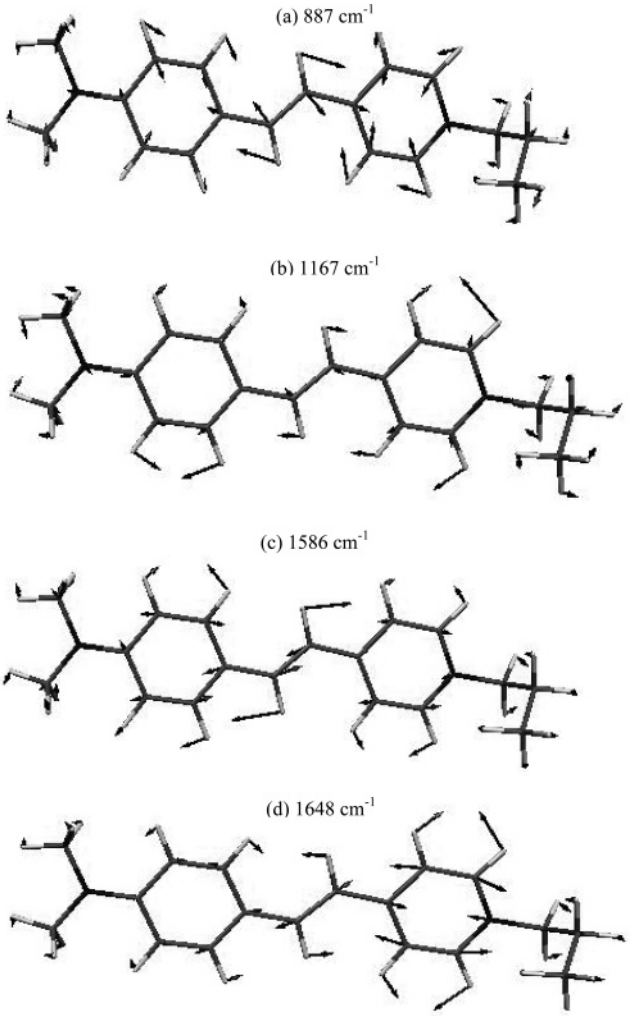

Figure 5. Normal-mode displacements of (a) 887, (b) 1167, (c) 1586, and (d) 1648 cm^{-1} vibrations.

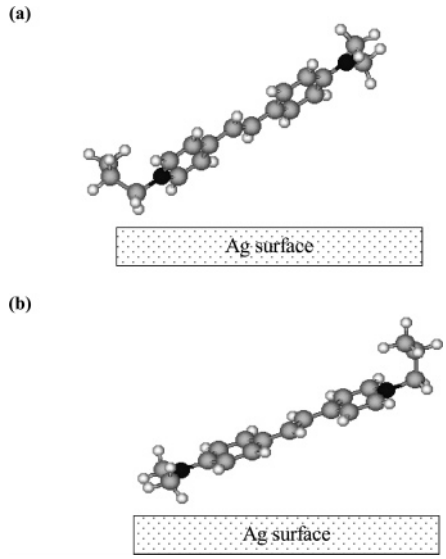

Figure 6. Schematic model of HC adsorbed on the silver surface (a) bound through the pyridyl ring and (b) bound via the dimethylamino group.

modes, a few weak bands, which are not observed in RRS, are observed in the SERRS spectrum, viz. 459, 501, 545, 585, 738, 848, 970, 1049, 1303, 1466, and 1507 cm^{-1}. All of these vibrations are in reasonable agreement with the IR and Raman data of methyl pyridinium iodide in the solid state and with the calculated vibrations of the HC−Ag complex. In the SERRS spectrum of HC, in addition to the relative enhancement of intensities of various vibrations in the region of 400−1700 cm^{-1}, the fluorescence background is also quenched due to the binding of the HC molecule with the silver surface.

The SERRS spectrum of hemicyanine, as shown in Figure 2c, is characterized by the presence of intense bands at 1161 and 1578 cm^{-1}, assigned to the $C_{34}N_{33}$ + pyridyl ring (CC) and C_2C_1 + aniline ring (CC) stretching vibrations, respectively. Many other ip Raman bands with moderate intensities are observed. The bands at 459, 545, 585, and 848 cm^{-1}, which arise from the oop deformations of the aromatic rings, are also observed. Of these modes, the 848 cm^{-1} band is assigned to the CH oop deformation of the aniline ring, pyridyl ring, and ethylene. In addition, a shoulder at 241 cm^{-1} (Figure 2c, inset) is observed, which is attributed to the Ag−N stretching vibration. This indicates that the adsorption of HC on the silver surface occurs via the nonbonding electrons of the nitrogen atom in the pyridyl ring or the aniline ring. HC, with its two nitrogen atoms (N_{14} and N_{33}), can be chemisorbed on to the silver surface via either of the N atoms or both can be involved in binding. To find out the most probable active site, the Mulliken charge densities on each atom were calculated from the B3LYP method using the 6-31G* basis set. The Mulliken charge densities, with hydrogens summed into heavy atoms, show that at the optimized geometry, the negative charge density on N_{14} and N_{33} atoms are −0.4659 and −0.3843, respectively. Thus, it is possible that the adsorption on the silver surface occurs through the nitrogen atom of the dimethylamino group or the pyridyl group. This is supported by the B3LYP/LANL2DZ calculations carried out for the *trans*-HC−Ag complex. The theoretical results show two stable conformers, I and II (Figure 6 a,b). In conformer I, the silver atom interacts with the pyridinium moiety, whereas in conformer II, the silver interacts with the dimethylamino group. However, the calculated results show that conformer I is slightly more favorable in energy as compared to conformer II. Because, the energy difference between the two conformers is quite low (138 cm^{-1}), it is expected that on the silver surface, both of the conformers exist.

The orientation of the adsorbate on the metal surface usually depends on the active sites of the molecule through which the interaction takes place and can be estimated from the enhancement of the relevant Raman bands according to the electromagnetic surface-selection rules. These surface-selection rules are known to be applicable under off-resonance conditions but can also be extended to preresonance and resonance conditions.[13,41] Although, under resonance conditions, there could be interference from the resonance-enhancement effect that could override the surface-selection rules. However, in the present study, to investigate the effect of the orientation and interaction of HC with the silver surface, the SERRS spectrum is compared to the RR spectrum instead of the normal Raman spectrum. This is expected to take the resonance-enhancement effect into consideration and, hence, would not interfere with the surface-selection rules. It is known from the surface-selection rules that any vibrational mode with its normal-mode component perpendicular to the metal surface is likely to show enhancement as compared to the parallel component. In cases where oop modes are also observed along with the enhanced ip vibrations, the molecule assumes a slightly tilted orientation with respect to the metal surface.[13,15,42] As mentioned earlier, the SERRS spectra of HC shows enhancement along various ip and oop stretching and bending vibrations. Thus, HC is bound to the metal surface

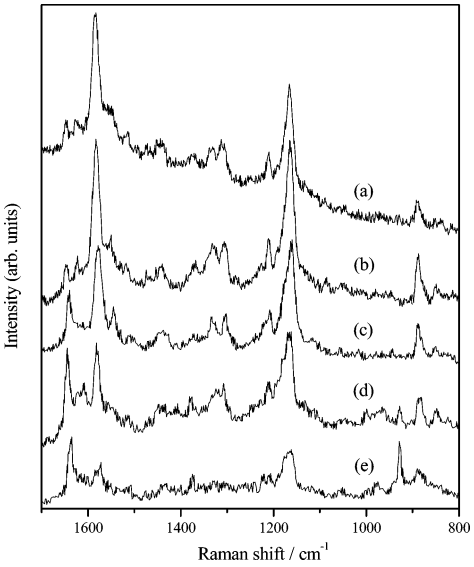

Figure 7. Effect of concentration on the SERRS spectra of HC (a) 2.4×10^{-5}, (b) 1.6×10^{-5}, (c) 1.3×10^{-5}, (d) 1.0×10^{-5}, and (e) 8×10^{-6} M.

through the nitrogen atom of the pyridyl ring or the dimethylamino group with the orientation being tilted with respect to silver surface.

The enhancement in SERRS spectra of HC is accompanied by a red-shift with no change in bandwidth along various Raman vibrations. Usually the red-shift ($\sim$10 cm^{-1}), accompanied with a substantial increase in the bandwidth, is observed in the case of aromatic molecules that are adsorbed on the metal surface via their π-systems.[43] Hence, the red-shift of 5−8 cm^{-1}, observed in the SERRS spectra of HC along various vibrations, viz. the 1578, 1167 cm^{-1} etc. with no change in bandwidth, suggests chemisorption of the HC molecule over the silver surface with a tilted orientation.

4.6. Effect of Concentration on the SERRS Spectra. In the present study, we have investigated the effect of concentration of the hemicyanine dye adsorbed on the silver surface. The SERRS spectra at different concentrations of HC, viz. 2.4×10^{-5}, 1.6×10^{-5}, 1.3×10^{-5}, 1.0×10^{-5}, and 8×10^{-6} M in the silver sol, are shown in Figure 7a−e. From the figure, it is seen that maximum intensity enhancement is observed at a HC concentration of 1.6×10^{-5} M (Figure 7b). With a further increase in HC concentration, it is observed that the intensities of the Raman bands decrease (Figure 7a) with an increase in the fluorescence background. It is also evident from Figure 7c−e that with lowering in HC concentration, although the Raman intensities decrease, the band at 1640 cm^{-1} shows relative enhancement with respect to the 1578 cm^{-1} mode. The modes at 1578 and 1640 cm^{-1} are assigned to the ethylene C_2C_1 + aniline ring stretches and pyridyl ring stretch, respectively. At a low concentration of HC, the Raman bands at 883 and 1161 cm^{-1}, which are mainly due to the contributions from the pyridyl ring stretch, tend to broaden out. This suggests that at a low concentration of the HC dye, the pyridyl ring interacts more effectively with the surface. This is possible only if the tilt angle becomes so large that the molecule is almost lying flat on the surface. This observation suggests that there is a change in the orientation of the adsorbate with a decrease in the HC concentration. This result corroborates the earlier observation.[16,42,44] The SERRS spectra shows that maximum enhancement is observed when a monolayer of the adsorbed species is formed on the surface, and with the formation of multilayers, the SERRS signal decreases with an increase in the fluorescence background. The monolayer of the HC dye is formed on the silver surface at a concentration of $\sim 1.6 \times 10^{-5}$ M, thus showing maximum enhancement in Raman intensities.

5. Conclusion

RR, SERRS, and theoretical (DFT calculations with B3LYP functional and CIS method with 6-31G* and LANL2DZ basis sets) studies have been investigated for the HC dye. The SERRS spectrum is compared to the RR data and is assigned on the basis of DFT calculations. The assignments for a few vibrational modes, particularly 887 and 1167 cm^{-1}, were found to be in disagreement with those reported earlier for a similar hemicyanine dye (methylpyridinium iodide[1]). The SERRS study shows the appearance of a shoulder at 241 cm^{-1} (Ag−N stretching vibration) along with the enhancement of various in-plane and a few out-of-plane vibrations. This suggests that the dye is chemisorbed on the silver surface through the nitrogen atom of the pyridyl or the dimethylamino group with a tilted orientation, which is also supported by the theoretical results. The observed red-shift of 4−8 cm^{-1} in the SERRS spectra along various vibrations indicates a strong interaction of HC on the silver surface. With the decrease in HC concentration, the SERRS spectra show intensity variations followed by an increase in the bandwidth of the pyridyl ring vibrations, which is attributed to an increase in the tilt angle of the molecule assuming a nearly flat orientation on the silver surface.

Acknowledgment. We thank Dr. S. M. Sharma, Head, Synchrotron Radiation Section, BARC, for his support and encouragement.

References and Notes

(1) Cao, X.; McHale, J. L. *J. Chem. Phys.* **1998**, *109*, 1901.
(2) Myers, A. B. In *Laser Techniques in Chemistry*; Myers, A. B., Rizzo, T. R., Eds.; Wiley: New York, 1995; Vol. 23, p 325; Myers, A. B. *Acc. Chem. Res.* **1997**, *30*, 519; Myers, A. B. *Chem. Rev.* **1996**, *96*, 911; Myers, A. B. *J. Raman Spectrosc.* **1997**, *28*, 389.
(3) Myers, A. B.; Mathies, R. A. In *Biological Applications of Raman Spectroscopy*; Spiro, T. G., Ed.; Wiley: New York, 1987; Vol. 2, p 1.
(4) Zink, J. I.; Shin, K.-S. K. *Advances in Photochemistry;* Wiley: New York, 1991; Vol. 16, p 119.
(5) Biswas, N.; Umapathy, S. *J. Chem. Phys.* **2003**, *118*, 5526; Biswas, N.; Umapathy, S. *J. Chem. Phys.* **1997**, *107*, 7849; Biswas, N.; Abraham, B.; Umapathy, S. *J. Phys. Chem. A* **2002**, *106*, 9397.
(6) McHale, J. L. *Acc. Chem. Res.* **2001**, *34*, 265.
(7) Moskovits, M. *Rev. Mod. Phys.* **1985**, *57*, 783.
(8) Chang, R. K., Furtak, T. E., Eds. *Surface Enhanced Raman Scattering*; Plenum: New York, 1982.
(9) Campion, A.; Kambhampati, P. *Chem. Soc. Rev.* **1998**, *27*, 241.
(10) Kneipp, K.; Kneipp, H.; Itzkan, I.; Dasari, R. R.; Field, M. S. *Chem. Rev.* **1999**, *99*, 2957.
(11) Cotton, T. M. In *Spectroscopy of Surfaces*; Clark, R. J. H., Hester, R. E., Eds.; Wiley: New York, 1988; Chapter 3.
(12) Pettinger, B. In *Adsorption of Molecules at Metal Electrodes*, Lipkowski, J., Ross, P. N., Eds.; VCH Publishers: New York, 1992; Chapter 6.
(13) Bolboaca, M.; Iliescu, T.; Paizs, Cs.; Irimie, F. D.; Kiefer, W. *J. Phys. Chem. A* **2003**, *107*, 1811; Bolboaca, M.; Iliescu, T.; Kiefer, W. *Chem. Phys.* **2004**, *298*, 87.
(14) Pergolese, B.; Miranda, M. M.; Bigotto, A. *J. Phys. Chem. B* **2004**, 108, 5698.
(15) Thomas, S.; Biswas, N.; Venkateswaran, S.; Kapoor, S.; Naumov, S.; Mukherjee, T. *J. Phys. Chem. A* **2005**, *109*, 9928; Thomas, S.; Biswas, N.; Venkateswaran, S.; Kapoor, S.; D'Cunha, R.; Mukherjee, T. *Chem. Phys. Lett.* **2005**, *402*, 361; Thomas, S.; Venkateswaran, S.; Kapoor, S.; D'Cunha, R.; Mukherjee, T. *Spectrochim. Acta* **2004**, *A60*, 25.
(16) Moskovits, M.; Suh, J. S. *J. Phys. Chem.* **1988**, *92*, 6327; Moskovits, M.; Suh, J. S. *J. Phys. Chem.* **1984**, *88*, 5526, 1293; Moskovits, M.; Suh, J. S. *J. Chem. Phys.* **1982**, *77*, 4408; Moskovits, M.; Suh, J. S. *J. Am. Chem. Soc.* **1985**, *107*, 6826.
(17) Mullen, K. I.; Wang, D.; Crane, L. G.; Carron, K. T. *Spectroscopy* **1992**, *7*, 24.
(18) Jones, M. A.; Bohn, P. W. *Anal. Chem.* **2000**, *72*, 3776.

(19) Ephardt, H.; Fromherz, P. *J. Phys. Chem.* **1989**, *93*, 7717.
(20) Mishra, A.; Patel, S.; Behera, R. K.; Mishra, B. K.; Behera, G. B. *Bull. Chem. Soc. Jpn.* **1997**, *70*, 2913.
(21) Mishra, A.; Behera, P. K.; Behera, R. K.; Mishra, B. K.; Behera, G. B. *J. Photochem. Photobiol.* **1998**, *A116*, 79.
(22) Chemla, D. S.; Zyss, J. *Nonlinear Optical Properties of Organic Molecules and Crystals*; Academic Press: Orlando, 1987.
(23) Kim, O.-K.; Choi, L.-S.; Zhang, H.-Y.; He, X.-H.; Shih, Y.-H. *J. Am. Chem. Soc.* **1996**, *118*, 12220.
(24) Ashwell, G. J.; Jackson, P. D.; Crossland, W. A. *Nature* **1994**, *368*, 438.
(25) He, G. S.; Bhawalkar, J. D.; Zhao, C. F.; Prasad, P. N. *Appl. Phys. Lett.* **1995**, *67*, 2433.
(26) Abraham, U. *An Introduction to Ultrathin Organic Films: From Langmuir-Blodgett to Self-Assembly*; Academic Press: Boston, 1991.
(27) Mishra, A.; Behera, R. K.; Behera, P. K.; Mishra, B. K.; Behera, G. B. *Chem. Rev.* **2000**, *100*, 1973.
(28) Mishra, A.; Behera, G. B.; Krishna, M. M. G.; Periasamy, N. *J. Lumin.* **2001**, *95*, 175.
(29) Huang, Y.; Cheng, T.; Li, F.; Luo, C.; Huang, C.-H.; Cai, Z.; Zeng, X.; Zhou, J. *J. Phys. Chem. B* **2002**, *106*, 10031.
(30) Shibasaki, K.; Itoh, K. *J. Raman Spectrosc.* **1991**, *22*, 753.
(31) Miranda, M.-M.; Puggelli, M.; Ricceri, R.; Gabrielli, G. *Langmuir* **1996**, *12*, 4417.
(32) Sahay, A. K.; Mishra, B. K.; Behera, G. B.; Shah, D. O. *Indian J. Chem., Sect. A: Inorg., Bio-inorg., Phys., Theor. Anal. Chem.* **1988**, *27*, 561.
(33) Mishra, A.; Behera, R. K.; Mishra, B. K.; Behera, G. B. *J. Photochem. Photobiol.* **1999**, *A121*, 63.
(34) Creighton, J. A.; Blatchford, C. G.; Albrecht, M. G. *J. Chem. Soc., Faraday Trans. 2* **1979**, *75*, 790.
(35) Kapoor, S. *Langmuir* **1998**, *14*, 1021.
(36) Frisch, M. J.; Trucks, G. W.; Schlegel, H. B.; Scuseria, G. E.; Robb, M. A.; Cheeseman, J. R.; Zakrzewski, V. G.; Montgomery, J. A., Jr.; Stratmann, R. E.; Burant, J. C.; Dapprich, S.; Millam, J. M.; Daniels, A. D.; Kudin, K. N.; Strain, M. C.; Farkas, O.; Tomasi, J.; Barone, V.; Cossi, M.; Cammi, R.; Mennucci, B.; Pomelli, C.; Adamo, C.; Clifford, S.; Ochterski, J.; Petersson, G. A.; Ayala, P. Y.; Cui, Q.; Morokuma, K.; Malick, D. K.; Rabuck, A. D.; Raghavachari, K.; Foresman, J. B.; Cioslowski, J.; Ortiz, J. V.; Stefanov, B. B.; Liu, G.; Liashenko, A.; Piskorz, P.; Komaromi, I.; Gomperts, R.; Martin, R. L.; Fox, D. J.; Keith, T.; Al-Laham, M. A.; Peng, C. Y.; Nanayakkara, A.; Gonzalez, C.; Challacombe, M.; Gill, P. M. W.; Johnson, B. G.; Chen, W.; Wong, M. W.; Andres, J. L.; Head-Gordon, M.; Replogle, E. S.; Pople, J. A. *Gaussian 98*, revision A.11.2; Gaussian, Inc.: Pittsburgh, PA, 2001.
(37) Becke, A. D. *J. Chem. Phys.* **1993**, *98*, 1372.
(38) Biswas, N.; Umapathy, S. *J. Phys. Chem. A* **1997**, *101*, 5555.
(39) Mohandas, P.; Umapathy, S. *J. Phys. Chem. A* **1997**, *101*, 4449.
(40) Cao, X.; Tolbert, R.; McHale, J. L.; Edwards, W. D. *J. Phys. Chem. A* **1998**, *102*, 2739.
(41) Miranda, M.-M.; Neto, N. *Colloids Surf., A* **2004**, *249*, 79.
(42) Pergolese, B.; Bigotto, A. *Spectrochim. Acta* **2001**, *A57*, 1191.
(43) Gao, P.; Weaver, M. J. *J. Phys. Chem.* **1985**, *89*, 5040.
(44) Chowdhury, J.; Ghosh, M. *J. Colloid Interface Sci.* **2004**, *277*, 121.